© Universiti Tun Hussein Onn Malaysia Publisher's Office

IJIE

Journal homepage: http://penerbit.uthm.edu.my/ojs/index.php/ijie
ISSN : 2229-838X e-ISSN : 2600-7916

The International Journal of Integrated Engineering

Hybrid Signal Processing and Machine Learning Algorithm for Adaptive Fault Classification of Wind Farm Integrated Transmission Line Protection

Osaji Emmanue[1*], Mohammad Lutfi Othman[1], Hashim Hizam[1], Muhammad M. Othman[2], Elhadi Aker[1], Okeke Chidiebere. A[1], T Nwagbara Samuel[1]

[1]Centre for Advanced Power and Energy Research and Department of Electrical and Electronics Engineering, Faculty of Engineering, Universiti Putra Malaysia, UPM Serdang, Selangor, 43300, Malaysia.

[2]Centre for Electrical Power Engineering Studies & Faculty of Electrical Engineering, Universiti Teknologi Mara Malaysia, Shah Alam, Selangor, Malaysia.

*Corresponding Author

DOI: https://doi.org/10.30880/ijie.2019.11.04.010
Received 17 April 2019; Accepted 8 July 2019; Available online 5 September 2019

Abstract: The technological advancement in integration of Renewable Green Energy Sources (RGES) like Wind Farm Generators (WFG), and Photovoltaic (PV) system into conventional power system as a future solution to meet the increase in global energy demands in order to reduce the cost of power generation, and improve on the climate change impact. This innovation also introduces challenges in the power system protection by it being compromised due to injected fault current infeeds on existing facilities. These infeed lead to the undesired trip of a healthy section of the line, and protection system failure. This paper presents a soft computational approach to adaptive fault classification model on High Voltage Transmission Line (HVTL) with and without RGES-WFG integration topologies, using extracted one-cycle fault signature of voltage and current signals with wavelet statistical approach in Matlab. The results are unique signatures across all fault types and fault distances with distinct entropy energy values on proposed network architecture. The supervised machine learning algorithm from Bayesian network classified 99.15 % faults correctly with the operation time of 0.01 s to produced best-generalized model with an RMS error value of 0.05 for single line-to-ground (SLG) fault identification and classification. Best suitable for adaptive unit protection scheme integration.

Keywords: Entropy energy, renewable green energy sources, Soft computation, wind farm generator, wavelet multiresolution

1. Introduction

The high cost of fossil fuel and global climate change impact of nonrenewable energy (NRE) generation sources has led to the integration of Renewable Green Energy Sources (RGES) in existing power system [1] [2][3]. The RGES are environmental friendly, cost-effective, and could be harnessed at low cost to meet the ever-increasing electrical energy demands, resulting from the explosive growth in world population as specified by the Global Wind Energy Council (GWEC) [4], [5]. The increase in WFG source integrations on existing transmission system has been implemented in countries like the U.S (with over 42% installed capacity), Europe (with 36% installed capacity), China, and Egypt [4]. The integration of RGES like Wind Farm Generator (WFG) and Photovoltaic (PV) systems on existing High Voltage Transmission Line (HVTL) grid, has compromised existing protection scheme coordination [6] [7]. This

*Corresponding author: osaji.emmanuel@gmail.com

led to wrong trips of a healthy section of the transmission lines, leading to undesired damages to equipment installations and personnel safety due to injected infeed current into the faulty section of the line affecting the already setting of the protection relays [8] [9].

These penetrations of RGES also come with some system challenge in term of reliability, security, stability and compromised power quality [10]. The need to provide a more robust protection scheme that is adaptive in nature towards meeting the current trend in the RGES paradigm shift is not only necessary but eminent [11]. This is particularly so, considering the limitations of both the fundamental units (e.g. differential, or pilot protection) involving total protection coverage of the transmission lines with the provision of high cost communication channels installations linking end sources, and the non-unit protection systems (e.g. distance relay) with partial line coverage protection schemes of HVTL [12]–[14]. This necessitate the need for a high-speed, low cost, and reliable unit protection scheme for the entire integrated WFG-HVTL protection scheme.

Currently, protections of different HVTL architectures have gone through series of developmental changes with the advent of Artificial Intelligence (AI), and soft computational Intelligence (CI) approaches [15]–[18]. A non-communication protection scheme with the deployment of high-speed Wavelet Multi-Resolution Analysis (WMRA) filter banks for fault transient current and voltage signal analysis has been proposed recently [6], [18]–[20]. These band filter extract of both high and low-frequency components of the measured fault signals and calculate the spectral energy of the two distinct measurement quantities by the relay in order to discriminate between the internal and external fault scenarios on the HVTL. A high-speed, low cost and reliable non-communication channel protection scheme for the entire unit protection of transmission lines have also been developed [21], [22]. Nevertheless, it is limited to fault current discrimination across transmission lines and cannot handle fault classifications, and location functions. An adaptive backup scheme has been proposed for fault location determination using a limited number of the phasor line voltage and current measurements from the backup protection zone [20], [23], [24]. An advanced signal processing analysis method of wavelet transform analysis of fault voltage and current waveforms recorded at a suitable monitoring location in the multi-bus meshed power system, to detect and classify faults has been proposed [25]. The robustness of improved adaptive protection proposed systems could not be guar-anteed, due to the few numbers of fault scenarios simulated in the research works. Fault identification, classifications, and location on a series compensated transmission line have also been developed using hybrid Wavelet-ANFIS algorithms, whereby wavelet feature extraction of one cycle fault voltage and current signals is per-formed based on norm entropy of decomposed signals. This deter-mines the main frequency, harmonics and transient features of the fault signals under various conditions [26], [27]–[30]. Earlier studies do not involve renewable energy sources integration on existing conventional line architectures in order to address the pending protections compromise challenges for during fault scenarios. This is considered as one major limitation that motivates this research work for further investigation into signature acquisition during fault occurrence.

In view of this limitation from previous work, a robust soft computational fault classification approach with detail comparative assessment study of Discrete Multiresolution Wavelet Analysis (DMRWA) on one-cycle voltage and current during faults for signals signature extraction and onward single line to ground (SLG) faults classification shall be performed so as to assess the HVTL protection scheme in the presence of WFG.

The article is organized with the Introduction section discussing the comparative advantages of the RGES against the conventionally known energy generation sources with respect to cost, environmental impact assessment and effects on existing protection schemes. The Methodology section divulges the proposed steps in meeting the objectives of the soft computational approach of DMRWA for the 11 fault signatures extraction and onward classification of SLG faults from one-cycle data with and without the integrated RGES. This is followed by the Result and Discussion section. Finally, the summary of the work and objectives fulfillment are discussed in the Conclusion section.

2. Methodology

The advent of smart grid technology requires an intelligent and automated fault detection and clearing operation scheme with little or no human interventions required [23]. This enhances protection and monitoring devices to be intelligently smart and adaptive in nature to faults or disturbances for data acquisition [24], faults classification and trip decision making when necessary [25]. This re-search work proposes an improved protection system dependability by preventing and eliminating faults as fast as possible with high precision, selectivity and reliability with minimal system interruptions or damages resulting from compromised protection safety system. This will be achieved with the application of soft computational approach (DMRWA) in extracting during-fault one-cycle signatures for accurate decision-making.

2.1 Unit protection

This paper present DMRWA feature extractions from one-cycle during fault transient voltage and current signals of HVTL system networks with and without integrated RGES-WFG upon fault inception on HVTL. A wideband spectrum of high frequency transient current signals at the fault location is created which propagates towards the substation bus bars. Other signals reflect back and forth in-between the faulted point and the system buses until a post-

fault steady state was attained [15], [26], [27]. This research proposes a dual-ended power generation sources on transmission line of 132kV, 50Hz, 200km HVTL with integrated 9MW RGES-WFG (with six units of 1.5 MW), and connected at the point of the com-mon couple bus bar (PCC) as displayed in Fig. 1. The Matlab Simulink Simulations scenarios of 11 faults types (AG, BG, CG, ABG, BCG, ACG, ABCG, AB, BC, AC, ABC) are executed across the transmission lines at selected fault locations (10, 30, 50, 70, 90, 110, 130, 150 and 190 km) with various fault inception angels (0, and 30), and fault resistances of 0.001Ω and 0.1 Ω. The fault signature from each scenario is extracted at a sampling frequency of 50 kHz from the PCC in order to eliminate the aliasing effect.

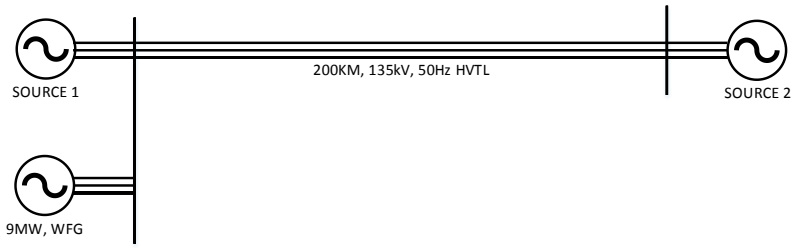

Fig. 1 - Wind farm generator integrated transmission line model

2.2 Wavelet Transform (WT)

Wavelet is small waveforms existing for a short time duration with an average value of zero and mostly adopted in advanced signal processing of transient signal analysis. This resolves analysis signal of fault transient signals into translated and scaled components of the applied mother wavelet function, as applied in previous transient signal analysis studies [28], [29]. The time-frequency localization benefits for little signal disturbances on HVTL, along with the unique ability to extract analyzed signal signatures for various frequencies bands and retaining the time function information are one of WT's unique benefits in fault transient studies.

The discrete multiresolution wavelet analysis (DMRWA) tool is made up of cascaded pairs of low and high-pass filter banks. The low pass filter (LPF) produced the mother wavelet function, while the high pass filter (HPF) produced the scaling function for the analysis. The extracted output coefficients of the LPF produced a high scale and low frequency (LF) coefficient contents of the analysis signal called 'approximate' (CA), and HPF extract high frequency (HF) but low scale coefficient contents called the 'detail' (CD) of the signal at the same level. This research adopted the Daubechies (db4) wavelets as the mother wavelet for the signal decomposition analysis to obtain the fundamental frequency of 50Hz using a sampling frequency of 50 kHz for flexibility in control and monitoring as displayed in 10th levels decomposition of extracted faults signals as displayed in Fig. 2.

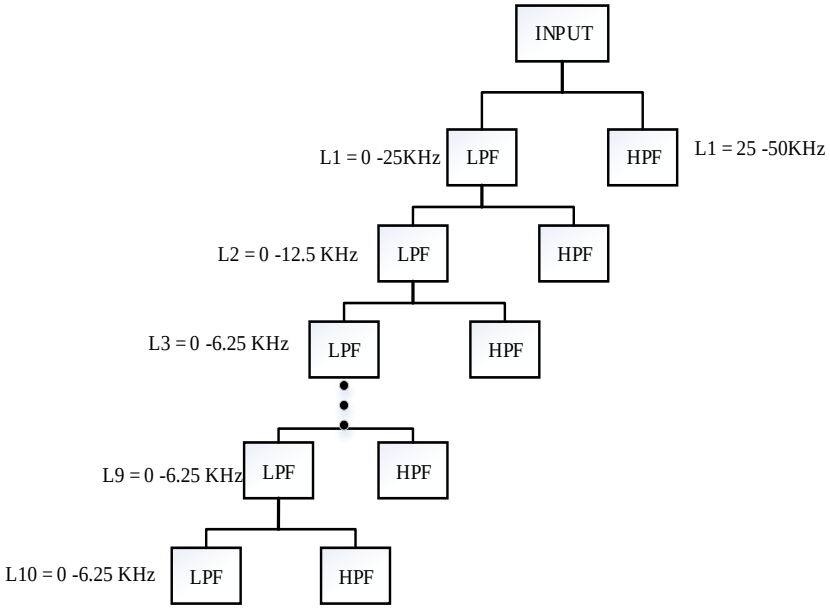

Fig 2 - Fault current decomposition filter banks

The db4 decomposes the transient fault signals from voltage and current into two equal halves of the frequency band at the first stage before passing each half through cascaded pair of filter banks of HPF and LPF. Unique signatures of CD and CA was then extraction at each level of decomposition. The output from the LPF is further decomposed in turns with another pair set of filters at sub-sequent levels until the need fundamental frequency band was attained as a display in Table 1. The CD from the HPF was discarded at every stage due to noise interferences in the high-frequency components.

Table 1- DMRWA decomposition scales

Levels	Detail coefficient (CD)	Frequency KHz	Approximate Coefficient CA	Frequency KHz
L1	D1	25 – 50 KHz	A1	0 – 25 KHz
L2	D2	12.5 – 25 KHz	A2	0 – 12.5 KHz
L3	D3	6.25 – 12.5 KHz	A3	0 – 6.25 KHz
L4	D4	3.125 – 6.25 KHz	A4	0 – 3.125 KHz
L5	D5	1.563 – 3.125 KHz	A5	0 – 1.5625 KHz
L6	D6	0.778 – 1.563 KHz	A6	0 – 0.78125 KHz
L7	D7	390.63 – 781.25 Hz	A7	0 – 390.63 Hz
L8	D8	195.31 – 390.63 Hz	A8	0 - 195.31 Hz
L9	D9	97.66 – 195.31 Hz	A9	0 – 97.66 Hz
L10	D10	48..83 – 97.66 Hz	A10	0 – 48.83 Hz

Samples of the SLG decomposed one-cycle during fault transient signatures of voltage and current signals as the most frequent and common transmission line fault at a 10km location with and without integrated WFG. The approximate components of both voltage and current signals at every level of decompositions contain unique signatures based on the signal standard deviation (STD), entropy energy (EE) and signal coefficients content. These features were further adopted for fault identification, and classification in an adaptive HVTL unit protection scheme design using different classification algorithm to determine the most accurate and fastest in execution speed for effective unit protection scheme. Figure 3 (a) and 3 (b) display comparative plots of decomposed voltage signal signatures of a SLG fault at 10km with and without RGES-WFG integration respectively. Similarly, the current signal decomposition display in Figure 4 (a) and 4 (b). The acronym A, B, C represent phase A, B, and C while for ground involvement in any fault scenario a capital letter G is used.

The EE of the decomposed fault voltage and current signals across SLG, LLG, and LLLG faults for both proposed network topologies indicates a decrease in values in the faulted voltage entropy energies for all the ground faults with the integration of the RGES-WFG topology, when compared with HVTL without RGES-WFG integration. On the other hand the current signal EEs increase with RGES-WFG integration as compared to normal power system topology across the entire ground fault as shown on the Table 2 to 3.

2.3 Adaptive SLG Fault Classification model

The statistical analysis of the decomposed approximate component at the 10th level presents the statistical relations such as min, max, STD and entropy energy (EE) of the signal for discriminate application on different signal attributes under both proposed power sys-tem topologies. The mathematical concepts and relationship between extracted signal signatures under both power network topologies are studied for unique modeling of adaptive fault identification, and classification that could be integrated into the existing protection relay to address the pending miss coordination challenges due to infeed contribution from the integrated RGES.

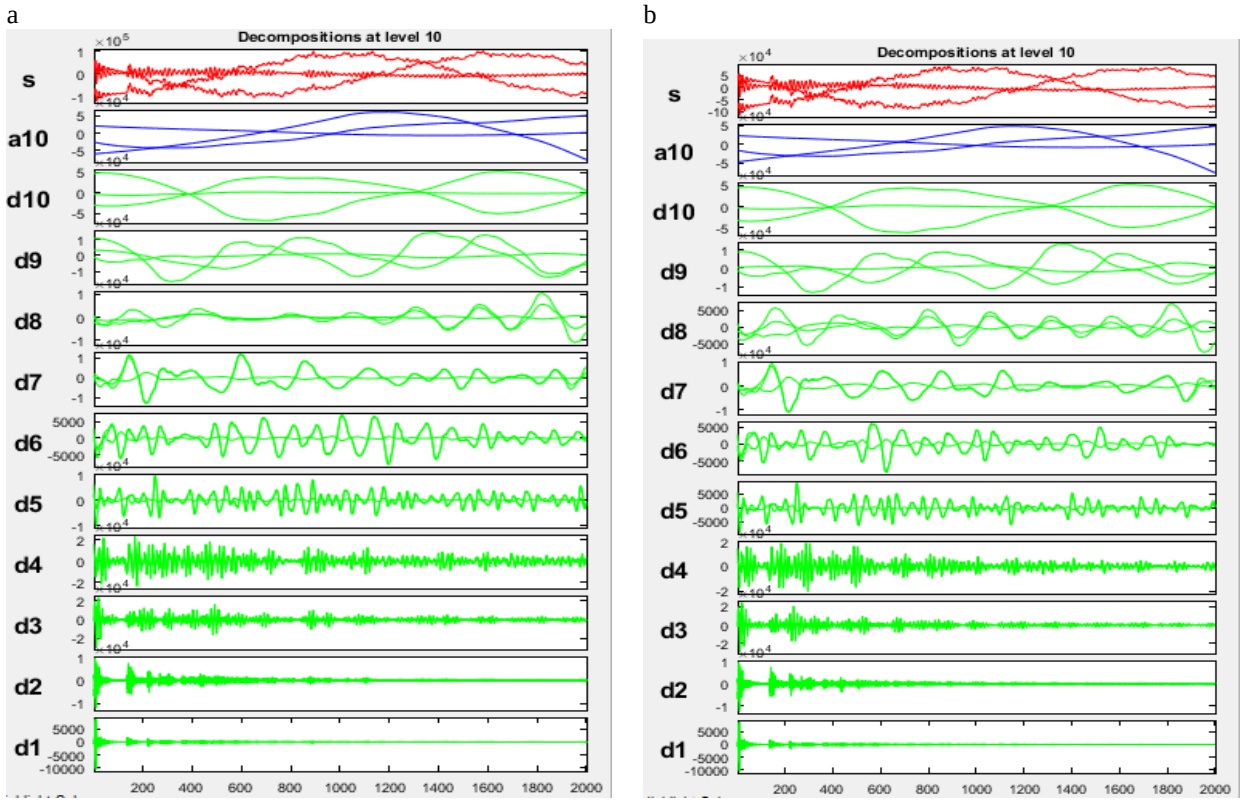

Fig. 3 - Voltage signal decomposition, (a) without WFG, (b) with WFG integrated at PCC

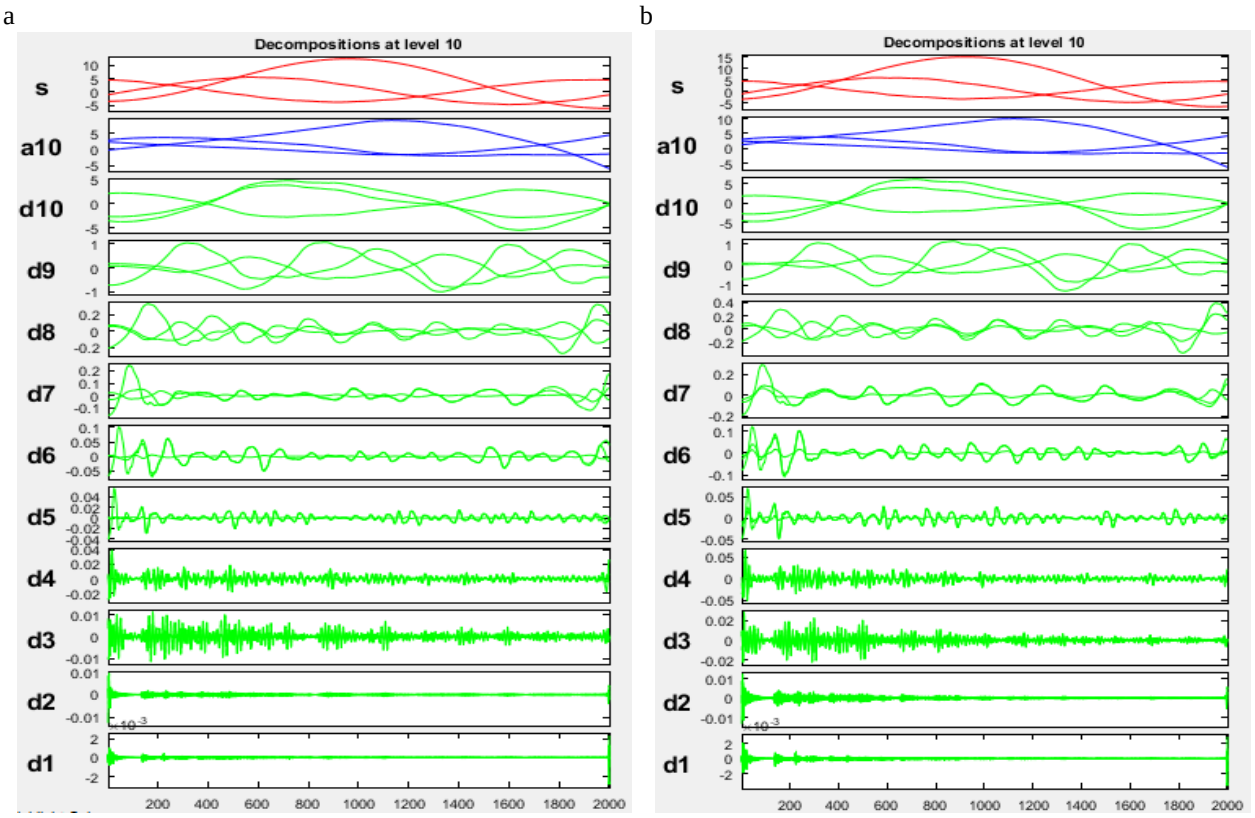

Fig. 4 - Current signal decomposition (a) without WFG, (b) with WFG integrated at PCC

The decomposed features of min, max EE, and STD of the original signal after passing through series of two-stage DMRWA filters at the last level produce unique detailed feature that was used to train and build an intelligent classifier models in order to enhance fast operational speed of unit protection adaptive relay with supervised classification approach as propose in this work.

The next stage in the adaptive relay development was the deployment of all extracted SLG fault signatures after decomposition of the fault current and the voltage signal for the supervised machine learning of a classification algorithm for effective predictions of SLG faults as the most common fault types on HVTL. 90% of the extracted features data was used for the training while 10% was deployed for the testing in order to validate the generalization of the classifier model.

3. Result and Discussions

The statistical min, max, and STD results presented from the de-composed faulted voltage and current signals measured at PCC for the same fault location, across 11 fault types show that the current infeeds penetrations from the integrated RGES increases the values of STD and EE from measured decomposed current comparison study of both power system topologies across all ground faults as displayed in Table 2 (a - b), and Table 3(a –b), except for the symmetrical LLLG fault result on Table 4. These unique values were deployed for individual fault type identification, to distinguish be-tween the ground fault from non-ground fault signatures using the one-cycle extracted fault voltage and current signals features. It can be observed that the STDs of the voltage signal have higher values as compared to those of the current signals for both network architectures under the same faulted conditions across all ground faults types (SLG, LLG, and LLLG).

Table 5 (a), 5 (b) and 6 display the obtained EE across both propose network topologies for SLG, LLG and LL faults across the entire HVTL, with a fault location at a step size of 20 km intervals. This produced far much higher values of EE with in feeds penetrations due to RGES -WFG integration on the line. The SLG faults have lower STD values as compared to double-line-to-ground (LLG) faults, while the LLLG fault has the highest STD.

Table 2(a) - SLG fault decomposition results at 10km

Fault		HVTL STATISTIC WITHOUT WFG			
Types	**Sig.**	**Min (-)**	**Max**	**STD**	**EE**
Phase	V	3.99+4	4.07+04	9290	7.54+12
AG	I	6.13	12.39	6.18	2.60+05
Phase	V	8.26+04	7.61+04	1.51+04	3.16+13
BG	I	8.08	9.13	6.07	2.28+05
Phase	V	3.62+04	4.28+04	9108	8.46+12
CG	I	12.48	3.33	5.58	1.30+05

Table 2(b) - SLG fault decomposition results at 10km

Fault		HVTL STATISTICS WITH WFG			
type	**Sig**	**Min (-)**	**Max**	**STD**	**EE**
Phase	V	3.78+04	4.16+04	9851	7.93+12
AG	I	6.594	14.90	7.29	3.30+05
Phase	V	8.14+04	6.96+04	1.40+04	3.09+13
BG	I	9.170	10.73	7.01	2.52+05
Phase	V	3.18+04	3.18+04	9490	7.78+13
CG	I	15.16	3.12	6.52	1.94+05

Table 3(a) - LLG fault decomposition results at 10km

Fault		HVTL STATISTIC WITHOUT WFG			
Types	**Sig**	**Min (-)**	**Max**	**STD**	**EE**
Phase	V	8.25+04	7.45+04	1.20+04	1.75+13
ABG	I	7.43	10.82	6.285	2.51+05
Phase	V	8.12+04	11.34+04	1.19+04	1.79+13
BCG	I	10.33	6.629	5.98	1.83+05
Phase	V	3.82+04	5.14+04	9.74+04	8.53+13
ACG	I	9.50	8.079	6.04	2.07+05

Table 3(b) - LLG fault decomposition results at 10km

Fault		HVTL STATISTICS WITH WFG			
Types	**Sig**	**Min (-)**	**Max**	**STD**	**EE**
Phase	V	7.819+04	6.649+04	1.043+04	1.730+13
ABG	I	7.0385	12.512	6.671	2.740+05
Phase	V	7.769+04	6.692+04	1.043+04	1.730+13
BCG	I	11.999	6.399	6.506	2.170+05
Phase	V	5.656+04	5.853+04	3.050+04	1.266+13
ACG	I	6.799	5.526	4.221	1.222+05

Table 4(a) - LLLG fault decomposition results at 10km

Fault Types	Sig	HVTL STATISTIC WITHOUT WFG Min	Max	STD	EE
ABCG	V	-5.55+04	5.55+04	5.346	1.38+13
	I	-9.241	8.67	6.212	2.19

Table 4(b) - LLLG fault decomposition results at 10km

Fault Types	Sig	HVTL STATISTICS WITH WFG Min (-)	Max	STD	EE
ABCG	V	-5.28+04	5.28+04	7.065	1.345+13
	I	-9.157	8.58	6.1717	2.159+05

The major difference lies in the discrimination of the STD values obtained from the RGES-WFG integration, having a much greater value for both voltage and current signals as compared to those obtained earlier without RGES-WFG integration. This major difference can be employed in the fault classifications across varying network topologies. This variation in wavelet statistical STD values resulted from the injection infeed contribution from the connected RGE-WFG integration. The faulted phase signal statistical values from both network topologies are also distinct for the symmetrical LLLG fault in Table 7.

The Table 8 result from the SLG classification model across six different classification algorithm from different categorized groups; the Rules functions adopted some set of rules formation based on the numerical data provided across feature attributes for the training of an intelligent device using either the most valuable attributes with the highest information relevance as seen in Rule.OneR classifier algorithm or allowing all attributes to contributes equally as seen in Rules.ZeroR algorithm. Another adopted tree algorithm category involves splitting all features to search for best feature with most useful information for prediction. The functions classifier adopted the Multilayer. Perceptron, Input. Mapping and Logistic classifier algorithm for the intelligent prediction using a supervised machine learning approach of mapping the input features to the predicted output

Finally, the Bayes Network category is a statistical probabilistic approach of classification, which indicated the best-generalized performance from the Bayesian network algorithms with 99.15 % correct classification performance. This model was also able to discriminate SLG fault under the two proposed network topologies RGES-WFG integration and without. This will address the pending protection limitations due to the Miro-grid integration impact on the currently existing system. The operation speed of the model is also fast enough for effective response time for trip command signal to associated breaker for effective reliability and system dependability.

Table 5(a) - SLG fault current entropy (EE) across the HVTL

Distance	Phase AG Fault E E(10^{05}) Without WFG	With WFG	Phase BG Faults EE (10^{05}) Without WFG	With WFG	Phase CG Faults EE (10^{05}) Without WFG	With WFG
10	2.605	3.296	2.284	2.516	1.297	1.9400
30	1.319	2.437	2.031	2.095	0.962	1.2720
50	1.826	1.967	1.868	1.865	0.763	0.9249
70	1.650	1.691	1.764	1.728	0.630	0.3755
90	1.504	1.506	1.697	1.639	0.537	0.5896
110	1.418	1.292	1.652	1.580	0.472	0.5025
130	1.319	1.302	1.599	1.540	0.429	0.4150
150	1.257	1.230	1.567	1.506	0.397	0.4020
170	1.223	1.185	1.551	1.487	0.374	0.3755
190	1.223	1.147	1.556	1.475	0.365	0.3652

Table 5(b) - LLG fault current entropy (EE) across the HVTL

Distance	Phase ABG Fault EE (10^{05})		Phase BCG Faults EE (10^{05})		Phase ACG Faults EE (10^{05})	
	Without WFG	With WFG	Without WFG	With WFG	Without WFG	With WFG
10	2.511	2.740	1.833	2.170	2.066	1.222
30	2.216	2.256	1.596	1.701	1.783	1.161
50	2.022	1.999	1.443	1.476	1.58	1.222
70	1.850	1.814	1.335	1.335	1.412	1.222
90	1.763	1.686	1.251	1.238	1.293	1.222
110	1.672	1.587	1.187	1.171	1.192	1.170
130	1.594	1.509	1.137	1.113	1.105	1.077
150	1.498	1.45	1.099	1.070	1.025	1.006
170	1.467	1.399	1.061	1.035	0.972	0.943
190	1.422	1.357	1.029	1.005	0.918	0.890

.

Table 7: LLLG fault current entropy (EE) across the HVTL

Distance	ABCG Faults EE (10^{05})	
	Without WFG	With WFG
10	2.1937	2.1590
30	1.9683	1.9300
50	1.7933	1.7480
70	1.6402	1.6018
90	1.5371	1.4827
110	1.4419	1.3852
130	3.4743	1.3034
150	1.2707	1.2377
170	1.2249	1.1793
190	1.1733	1.1297

Table 8 - SLG Fault classified model

Applied classifier Algorithm	Correctly Classified (%)	Incorrectly classified (%)	RMS error	Time (s)
Rule ZeroR	16	83.54	0.373	0
Bayesian network	99.15	0.84	0.049	0.01
Rules.OneR	64.98	35.02	0.342	0.02
Multilaye Perceptron	86.92	13.08	0.183	1.01
Input.Mapping Classifier	16.46	83.54	0.373	0
Trees.RandomForest	100	0	0.062	1.013
Function.Logistic	89.03	10.97	0.199	0.38

4. Conclusions

This study have been able to provide an improved adaptive protection relay algorithm through a novel hybrid signal processing and supervised machine learning approach to solving the pending protection coordination challenges in RGES integration on existing conventional system to meeting the energy sustainability problem and reduction of the climate change effect from the GHG emission gases from conventional generation sources.

This study is limited to WFG micro-grid integration on the existing transmission line, future work can be explored with other natural green energy sources like the PV farm integration in areas where wind speed is not readily available or stable

Acknowledgement

I want to use this opportunity to acknowledge the cooperation I have always enjoyed from my supervisor, supervisory committee members and the Centre for Advanced Power and Energy Research of the Department of Electrical and Electronics Engineering, Faculty of Engineering, Universiti Putra Malaysia. Without whom this work would not have been possible.

References

[1] R. N. Fard and E. Tedeschi (2018). Integration of Distributed Energy Resources into Offshore and Subsea Grids. CPSS Trans. POWER Electron. Appl., 3, 36–45.

[2] Z. C. Zou, X. Y. Xiao, Y. F. Liu, Y. Zhang, and Y. H. Wang (2016). Integrated Protection of DFIG-Based Wind Turbine with a Resistive-Type SFCL under Symmetrical and Asymmetrical Faults. IEEE Trans. Appl. Supercond., 26, 7.

[3] P. Kong (2018). A Distributed Management Scheme for Energy Storage in a Smart Grid. IEEE Trans. Ind. INFORMATICS, 14, 1392–1402.

[4] H. Aoshima (2010). Wind Farm Protection Systems: State of the Art and Challenges," INTECH, 1, 266–289.

[5] V. Nelson, (2009). WIND ENERGY (Renewable Energy and the Environment). Taylor & Francis Group 6000 Broken Sound Parkway NW, Suite 300 Boca Raton, FL 33487-2742.

[6] B. K. Panigrahi, S. R. Samantaray, and R. Dubey (2016). Adaptive distance protection scheme for shunt-FACTS compensated line connecting wind farm. IET Gener. Transm. Distrib., 10, 247–256.

[7] L. Tripathy, M. K. Jena, and S. R. Samantaray (2014). Decision tree-induced fuzzy rule-based differential relaying for transmission line including unified power flow controller and wind-farms. IET Gener. Transm. Distrib., 8, 2144–2152.

[8] A. Esmaeilian, T. Popovic, and M. Kezunovic (2015). Transmission line relay mis-operation detection based on time-synchronized field data. Electr. Power Syst. Res., 125, 174–183.

[9] S. Chen, N. Tai, C. Fan, J. Liu, and S. Hong (2017). Adaptive distance protection for grounded fault of lines connected with doubly-fed induction generators. IET Gener. Transm. Distrib., 11, 1513–1520.

[10] B. K. Panigrahi, R. Dubey, and S. R. Samantaray (2014). Simultaneous impact of unified power flow controller and off-shore wind penetration on distance relay characteristics. IET Gener. Transm. Distrib., 8, 1869–1880.

[11] L. He, C. C. Liu, A. Pitto, and D. Cirio (2013). Distance Protection of AC Grid With HVDC- Connected Offshore Wind Generators. IEEE Trans. Power Deliv., 29, 1–9.
[12] D. Tzelepis et al., (2017). Single-ended differential protection in MTDC networks using optical sensors," IEEE Trans. Power Deliv. 32, 1605–1615.
[13] M. Biswal, (2016). Faulty phase selection for transmission line using integrated moving sum approach. IET Sci. Meas. Technol., 10, 61–767.
[14] F. E. Pérez, R. Aguilar, E. Orduña, J. Jäger, and G. Guidi (2012). High-speed non-unit transmission line protection using single-phase measurements and an adaptive wavelet: zone detection and fault classification. IET Gener. Transm. Distrib., 6, 593.
[15] M. K. Jena, S. R. Samantaray, S. Member, B. K. Panigrahi, and S. Member (2015). A New Wide-Area Backup Protection Scheme for Series-Compensated Transmission System. 11, 1–11.
[16] J. Ma, C. Liu, Y. Zhao, S. Kang, and J. S. Thorp (2016). An adaptive overload identification method based on complex phasor plane," IEEE Trans. Power Deliv., 31, 2250–2259.
[17] L. T. Lines, J. Wu, H. Li, G. Wang, and Y. Liang (2017). An Improved Traveling-Wave Protection Scheme. 32, 106–116.
[18] Z. Guo, S. Yang, W. Yu, L. Zhang, Z. Zhong, and Y. Sui (2018). Non-communication protection scheme for power transmission system based on transient currents, HHT and SVM. IET Gener. Transm. Distrib., 12, 2816–2824.
[19] A. Yadav and A. Swetapadma (2014). Improved first zone reach setting of artificial neural network-based directional relay for protection of double circuit transmission lines. IET Gener. Transm. Distrib., 8, 373–388.
[20] A. a. Hajjar (2013). A high speed noncommunication protection scheme for power transmission lines based on wavelet transform. Electr. Power Syst. Res., 96, 194–200.
[21] D. Tzelepis et al., (2017). Single-Ended Differential Protection in MTDC Networks Using Optical Sensors. 32, 1605–1615.
[22] M. K. Neyestanaki and A. M. Ranjbar (2015). An Adaptive PMU-Based Wide Area Backup Protection Scheme for Power Transmission Lines. IEEE Trans. Smart Grid, 6, 1550–1559.
[23] S. Som and S. R. Samantaray (2018). Efficient protection scheme for low-voltage DC micro-grid," IET Gener. Transm. Distrib., 12, 3322–3329.
[24] J. G. Rao and A. K. Pradhan (2017). Supervising distance relay during power swing using synchrophasor measurements," IET Gener. Transm. Distrib., 11, 4136–4145.
[25] Y. Usama, X. Lu, H. Imam, C. Sen, and N. C. Kar (2014). Design and implementation of a wavelet analysis-based shunt fault detection and identification module for transmission lines application. IET Gener. Transm. Distrib., 8, 431–441.
[26] B. Y. Vyas, B. Das, and R. P. Maheshwari (2016). Improved Fault Classification in Series Compensated Transmission Line: Comparative Evaluation of Chebyshev Neural Network Training Algorithms. IEEE Trans. Neural Networks Learn. Syst., 27, 1631–1642.
[27] B. Rathore and A. G. Shaik (2017). Wavelet-alienation based transmission line protection scheme. IET Gener. Transm. Distrib., 11, 995–1003.
[28] B. Y. Vyas, R. P. Maheshwari, and B. Das, "Improved fault analysis technique for protection of Thyristor controlled series compensated transmission line," Int. J. Electr. Power Energy Syst., vol. 55, pp. 321–330, 2014.
[29] A. R. Adly, R. A. El Sehiemy, A. Y. Abdelaziz, and N. M. A. Ayad (2016). Critical aspects on wavelet transforms based fault identification procedures in HV transmission line," IET Gener. Transm. Distrib., 10, 508–517.
[30] H. Seyedi and S. AsghariGovar (2016). Adaptive CWT-based transmission line differential protection scheme considering cross-country faults and CT saturation. IET Gener. Transm. Distrib., 10, 2035–2041.